Unconventional magnetic properties of $La_{1-x}Ba_xMnO_3$ thin films grown on $SrTiO_3(100)$ by metalorganic aerosol deposition

A. BELENCHUK[1], V. CANTSER[1], V. MOSHNYAGA[2], O. SAPOVAL[1], E. ZASAVITSKI[1]
[1]*Institute of the Electronic Engineering and Nanotechnologies "D. Ghitu", Academy of Sciences, Academiei str. 3/3, MD-2028 Chisinau, Moldova, belenchuk@iien.asm.md*
[2]*I. Physikalisches Institut, Georg-August-Universitat-Gottingen, Friedrich-Hund-Platz 1, D-37077 Gottingen, Germany, vmosnea@gwdg.de*

***Abstract* — Epitaxial $La_{1-x}Ba_xMnO_3$ thin films were grown on $SrTiO_3(100)$ substrates by metalorganic aerosol deposition technique. AFM surface analysis indicates a layer-by-layer growth mode. The occurrence of Laue thickness fringes in X-ray diffraction (XRD) spectra indicates a high quality single-crystalline growth of an uniformly strained film, whereas the X-ray reflection (XRR) reveals the presence of a few unit cells layer with modified electronic density. A high metal-insulator transition temperature, T_{MI}=335 K, as well inductive coupled plasma emission spectroscopy analysis indicate the formation of LBMO with optimal Ba doping *x*=0.32. However, from magnetization measurements a high Curie temperature, T_C=335 K, and a low coercitive field (30 Oe) coexist with a reduced saturation magnetization (~ 3 μ_B/Mn) and broadened para-ferromagnetic transition. The relevance of magnetic phase inhomogeneity can be further revealed from the low-temperature magnetization loops. We discuss the results within the concept of "dead magnetic layer" close to the film/substrate interface, which may lead to the coexistence of different magnetic phases in the "body" of the LBMO film.**

***Index Terms* — $La_{1-x}Ba_xMnO_3$ thin films, metal-organic aerosol deposition, layer-by-layer growth, transport and magnetic properties.**

I. INTRODUCTION

Perovskite-type colossal magnetoresistive manganites such as $La_{1-x}Ba_xMnO_3$ (LBMO) belong to the strongly correlated electron systems, which show a reach diversity of physical properties [1, 2]. Epitaxial growth of manganites has figured conspicuously in the search for new generations of electronic materials for information processing, data storage, and sensing [3]. All applications require manganite thin films with a smooth surface morphology, large magnetization, small residual resistivity, and sharp electric and magnetic transitions [4].

In this paper we demonstrate a metal-organic aerosol deposition growth and properties of LBMO thin films on the near perfect matched $SrTiO_3$ (STO) substrates. LBMO thin film was chosen since this compound appears to be one of the most attractive for device applications due to the high values of metal-insulator transition and Curie temperatures, $T_{MI}=T_C\sim340$ *K*, which both exceed the room temperature. Particularly interesting is the application of LBMO as a suitable material for uncooled bolometric detectors of the infrared radiation [5]. The presence of mechanic strain in thin oxide films is the crucial parameter to be optimized in their growth and electronic properties. LBMO films are expected to experience a small strain effect when grown on STO with optimal Ba-doping [6]. Moreover T_C was found to increase in a slightly tensile strained $La_{0.8}Ba_{0.2}MnO_3$ films grown on STO at about 0.3% mismatch [7].

Physical vapor deposition such as pulsed laser deposition is the most extensively used technique for the growth of complex oxide films. However, for a large-scale production of oxide films the metal-organic chemical vapor deposition (MOCVD) techniques seems to be more attractive [8]. Metalorganic aerosol deposition (MAD) technique [9] as one of the promising modifications of the liquid delivery MOCVD was used in this study.

The aim was to optimize the MAD growth parameters and, thus, to fabricate a high quality LBMO/STO films with atomically smooth surface and optimal composition (Ba-doping).

II. EXPERIMENTS

$SrTiO_3(100)$ substrates from "Crystec GmbH" were used for the present study. TiO_2-terminated surface with 100-200 nm wide terraces and straight single unit cell ledges was prepared by immersing the substrate in water, followed by etching in NH_4F buffered HF solution and by annealing at 950ºC during 1 hour [10].

Epitaxial growth of LBMO films was performed in a custom-built MAD system, equipped by pneumatic nozzles and peristaltic pumps for the feeding of precursor solution. The films were deposited at a substrate temperature, T_S=870-950ºC, at a constant deposition rate ~1.5 Å/s. The precursors, β-diketotates of La^{3+}, Ba^{2+} and Mn^{2+}, have been dissolved in dimethylformamide to obtain a solution with the molar Mn concentration of 0.015M. The solution composition has been varied to adjust the level of Ba-doping as well as to obtain equal ratio between cations that is required to prevent a formation of precipitates.

The film surface morphology was characterized by atomic force microscopy (AFM) at room temperature in a

This work was supported by DFG (SFB 602) and STCU grant 5390.

Veeco Multimode V Scanning Probe Microscope. The film thickness was determined by a small-angle x-ray scattering (SAXS) in a Brucker D8 diffractometer. X-ray diffraction (XRD) was performed in a Siemens D5000 diffractometer. Four-probe resistance measurements by using silver paste contacts were performed in a He cryostat. Magnetization as a function of temperature and magnetic field was measured by using Quantum Design MPMS SQUID magnetometer.

III. RESULTS AND DISCUSSION

Fig. 1 shows an AFM 5×5 μm image of a 33 nm thick LBMO film grown from optimized precursor composition at T_S=915ºC with deposition rate 1,37 Å/s. The monolayer step and terrace structure is clearly visible. The one-unit-cell-height islands, observed on the terraces, indicate a "layer-by-layer" growth mode rather than the "step-flow" growth. The terrace width is approximately equal to that of STO substrate surface and the root-mean-square roughness (RMS) of the film samples is very small, RMS=0.12 nm. Precipitates, related to the off-stoichiometric deposition, were not observed for these growth conditions and composition of precursors in solution, indicating a stochiometric (equal) ratio between A- and B-cations.

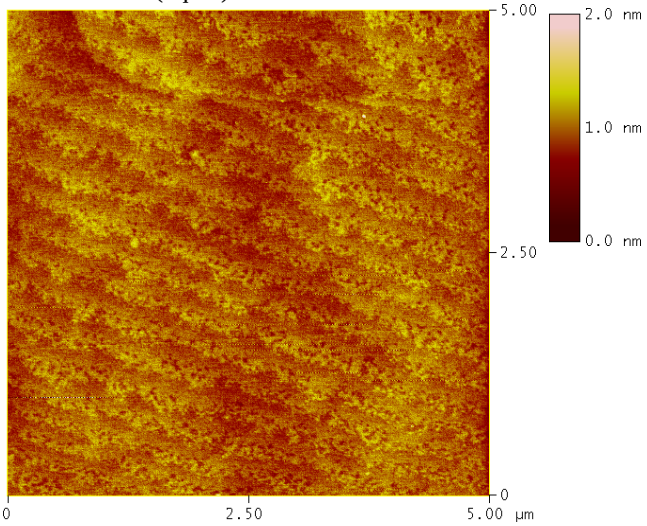

Fig. 1. AFM image of a 33 nm thick LBMO film grown on $SrTiO_3$(100).

The film thickness of each sample was determined from the interference fringes in the respective SAXS curve, using the relation $t = \lambda/(2\Delta\omega)$, where λ is the CuK_α x-ray wavelength and Δω is the oscillation angular period. In Fig. 2 we present the SAXS pattern of a LBMO film, grown at the same optimized growth conditions and precursor composition. The small-period oscillations (Kiessig fringes) due to the total film thickness were observed up to 6 degrees, confirming both the smoothness of the film surface and substrate/film interface. However, the damping of the interference fringes is not regular undergoing by bending at about 2.8º. This bending indicates the presence of oscillations with a longer period, originated from a very thin layer. Therefore SAXS data clearly reveal a two-layer structure of the LBMO film. The total thickness of LBMO film is 32,8 nm, whereas the thickness of the thin intermediate layer was estimated from the angle of bending to be ~3 nm. It is necessary to note that most of other samples, even fabricated at not optimal conditions, also exhibit a similar SAXS features, indicating a persistent formation of LBMO films with a two-layer structure.

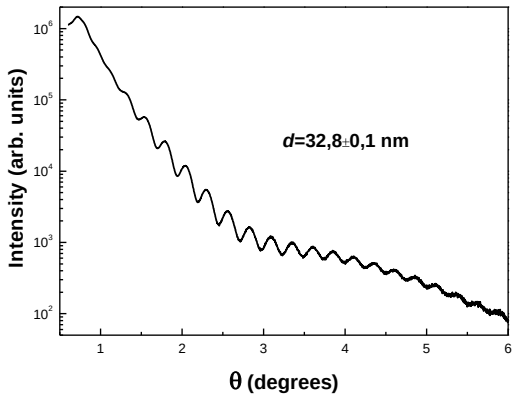

Fig. 2. X-ray reflectivity curve of LBMO film grown on $SrTiO_3$(100) with layer-by-layer growth mode.

The bulk LBMO for the optimal Ba-doping, *x*~0.33, can be considered as a pseudocubic perovskite with the lattice parameter, c=3.910 Å, thus leading to the lattice mismatch of +0.15% with STO substrate [6]. Since this compressive strain is small the LBMO films have to be uniformly strained being grown on STO. The XRD analysis confirms growth of LBMO films with no strain gradient. Fig. 3 shows the XRD pattern around the (001) STO Bragg peak. The out-of-plane lattice parameter of the LBMO film could not be calculated with a high precision due to the overlap of the film peak with the substrate peak. Next to the substrate (001) peak, a finite thickness fringes (Laue fringes) were observed with the period corresponding well to the film thickness t=33 nm, calculated from SAXS. The clear fringes indicate a high quality sample with smooth surface and substrate/film interface, confirming the AFM and SAXS data. The Laue fringes also infer a high crystal quality of the coherently strained LBMO film.

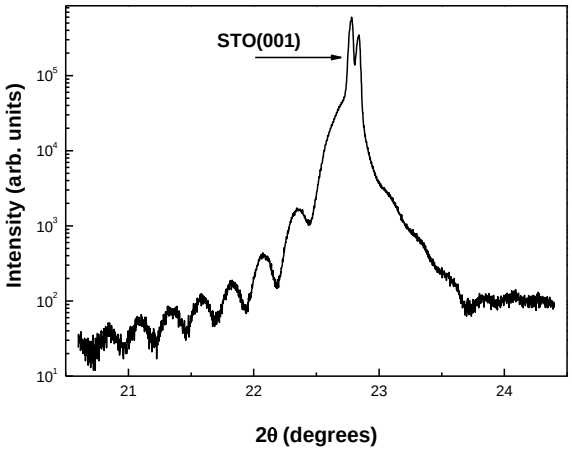

Fig. 1. X-ray diffraction scan of a 33 nm LBMO film grown on $SrTiO_3$(100) substrate. The substrate (001) Bragg peak overlaps with the corresponding film peak, and thickness fringes are observed.

A strong overlap of the film (002)-peak with the

STO(001) peak makes impossible the estimation of LBMO composition from the value of lattice parameter constant. The cation ratios were evaluated with a high precision by means of inductive coupling plasma (ICP) emission spectroscopy. For the sample prepared at exactly the same processing conditions (precursor composition, substrate temperature and growth rate) the ICP analysis results in a content of Ba x=0.32, which is very close to the optimal doping level.

It is known the lattice constant of $La_{0.68}Ba_{0.32}MnO_3$ grown on STO is equal to 3.909 Å [6]. But the out-of-plane lattice parameter of thin films has to be larger than the bulk value due to compressive strain, which shortens the in-plane parameter and elongates the out-of-plane parameter. Accepting a constant volume of the unit cell, the value of the out-of-plane lattice parameter is then c=3.917 Å for the sample analyzed by ICP.

The functional properties of LBMO films such as electric transport and magnetization are represented here for the same 33 nm thick LBMO film grown at optimal conditions.

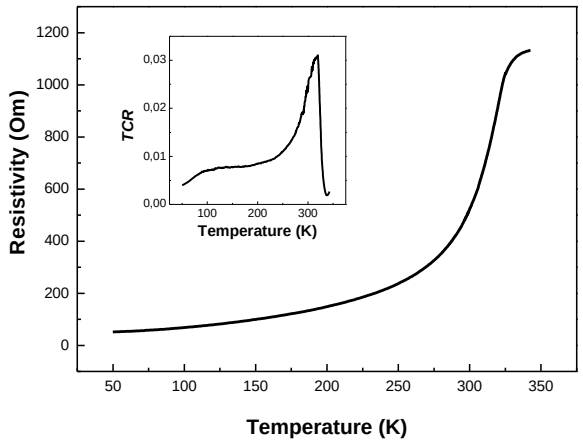

Fig. 2. Temperature-dependent resistivity of 33 nm thick LBMO film grown on SrTiO3(100). The inset shows temperature dependence of *TCR=(dR/dT)/R*.

The temperature-dependent resistivity, shown in Fig. 4, reveals metallic behavior starting from T=342 K, which was our highest temperature for the used experimental setup. Taking into consideration the slope of the R(T) curve at the starting temperature, it can be concluded that the resistivity peak and, respectively, the temperature of the metal-insulator transition, T_{MI}, should be well above 342 K. The value of T_{MI} of the LBMO film corresponds to the previously reported results for the bulk LBMO single crystal material. However, the residual resistivity for this LBMO/STO at 50K is ρ_{res}=350 μΩcm is several times higher than the best values ρ_{res}~70 μΩcm, obtained for the epitaxial manganite films e.g. LSMO on STO [4]. The inset in Fig. 4 represents the temperature coefficient of the resistance, *TCR=(dR/dT)/R*, as a function of temperature. The maximum value of *TCR*=3.1 %/K, observed at T=319K, indicates that LBMO/STO film might be interesting for the application as an uncooled bolometer material due to relatively high *TCR* values close to room temperature.

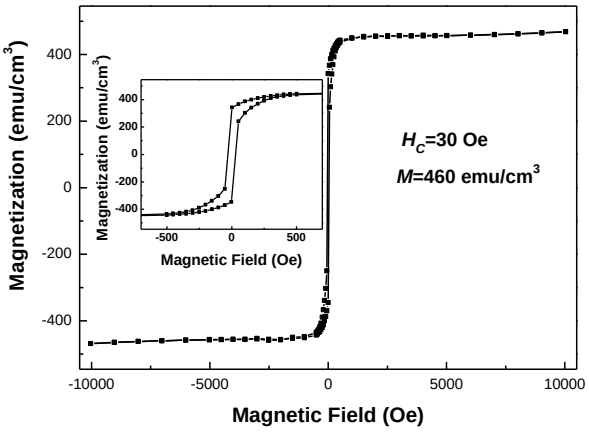

Fig. 3. Field dependence of the magnetization obtained at 10K with the field applied in the plane of 33 nm LBMO film on $SrTiO_3$(100). Inset shows the same hysteresis loop at low magnetic fields.

Fig. 5 shows the low temperature (10 K) magnetic moment loop without subtraction of diamagnetic background from the STO substrate. The saturation magnetization, M≈460 emu/cm^3 (≈3 μ_B/Mn), evaluated for magnetic field, H≈500 Oe, is significantly smaller than it can be expected for the optimally doped manganite, which should possess M~3.7μ_B/Mn. This indicates that the film material is magnetically inhomogeneous and contains an additional magnetic phase with reduced magnetization. This inhomogeneous magnetic structure of the LBMO film masks diamagnetic contribution, originated from STO substrate. In addition to the main ferromagnetic phase the LBMO has to have a paramagnetic phase to compensate the diamagnetism from STO. In spite of complex magnetic structure the magnetization of LBMO is very soft with coercitive field, H_C≈30 Oe, that reflects high microstructural perfection (absence of pinning centers) of LBMO film on STO.

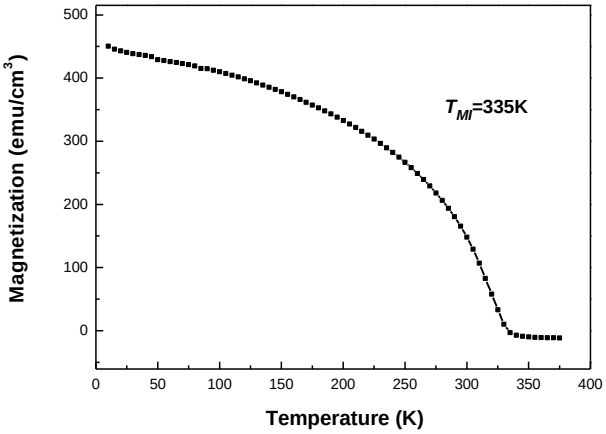

Fig. 4. Field cooled temperature dependence of the magnetization measured in external field H=1000 Oe for LBMO film on $SrTiO_3$(100).

A temperature dependence of magnetization, measured at H=1000 Oe after field-cooling (FC), is presented in Fig. 6. In spite of compressive strain that suppresses the

ferromagnetism by changing the occupancy of two e_g-orbitals the Curie temperature, T_C=335K, corresponds well to the values for LBMO with optimal Ba doping. However, the sharpness of the magnetic phase transition is relativity weak compared to the optimally doped manganites and, in addition, the temperature-dependent magnetization does not saturate at low temperatures. Both these features are in line with the above conclusion on the complicated (inhomogeneous) magnetic structure of LBMO/STO film.

IV. CONCLUSION

The appearance of Laue fringes in XRD patterns is known to be a pure diffraction-related phenomenon and a more clear fringes could be obtained if the difference between the lattice constants of the two materials is more pronounced that is no strain gradients exist. Alternatively, the Kiessig-fringes in SAXS arise due to the difference in the electron density of materials. Both XRD and SAXS data indicate an inhomogeneous distribution of the charge density along the surface normal to the film, whereas crystalline structure of the film is perfectly uniform across the film. Thus, although LBMO is structurally a single-layered film, the electronic distribution is not uniform, resulting in the formation of an intermediate layer with a thickness of a few i.e. 6-8 unit cells.

The occurrence of two-layer structure of $La_{0.7}Sr_{0.3}MnO_3$ was recently revealed in the films grown on STO [11]. The intermediate layer formation was explained by doping instabilities and/or charge transfer at the interface, resulting in the variation of the average Mn-valence from the mixed Mn^{3+}/Mn^{4+} to an enriched Mn^{3+} region near the substrate interface. The presence of a similar intermediate layer with changed average Mn-valence can explain unconventional magnetic properties of LBMO films, i.e. from one hand, a high transition temperature and small coercitivity and, from the other hand, a reduced value of magnetization and broadened magnetic transition. In contrast to the $La_{0.7}Sr_{0.3}MnO_3$/STO [11], in our LBMO/STO samples the intermediate layer appears to be compressively strained in the same manner as the "body" of the film.

Moreover, in our LBMO/STO films a reduction of the magnetization is too large to be explained by a thin intermediate layer with the thickness of few unit cells. It was recently shown that coherently strained $La_{0.6}Ca_{0.4}MnO_3$ film grown on $NdGaO_3$(100) substrate possess a very complicated magnetic structure contained two different ferromagnetic phases as well as a paramagnetic one [12]. Magnetic and electronic phase separation is commonly observed in many manganites even in the case of perfectly grown films without such structural defects as grain and twin boundaries. Epitaxial strains play especially significant role in the electric and magnetic phase separation for a high quality films. Thus, the complicated magnetic structure of $La_{0.6}Ca_{0.4}MnO_3$ [12] was emerged a result of stress relaxation in a small fraction of the film material. Manganites are disposed to contain small phase fractions that cannot be easily detected in many measurements. A detailed experimental study is required to understand the origin of the two-layer film configuration and of the bulk phase separation in coherently strained LBMO/STO films without extrinsic effects associated with grain or twin boundaries. The understanding and controlling the phase separation phenomenon is a key factor for the future improvement of the LBMO films functional properties and/or for the potential using of such minor phases in devices.

ACKNOWLEDGMENTS

The authors thank to C. Ballani for the IPC analysis of the film composition.

REFERENCES

[1] E. Dagotto, "Open questions in CMR manganites, relevance of clustered states and analogies with other compounds including the cuprates," *New Journal of Physics*, vol. 7, p. 67, 2005.

[2] Y. Tokura, "Critical features of colossal magnetoresistive manganites," *Reports on Progress in Physics*, vol. 69, p. 797, 2006.

[3] A. M. Haghiri-Gosnet and J. P. Renard, "CMR manganites: physics, thin films and devices," *Journal of Physics D: Applied Physics*, vol. 36, p. R127, 2003.

[4] H. Boschker and et al., "Optimized fabrication of high-quality $La_{0.67}Sr_{0.33}MnO_3$ thin films considering all essential characteristics," *Journal of Physics D: Applied Physics*, vol. 44, p. 205001, 2011.

[5] M. A. Todd, *et al.*, "Colossal magnetoresistive manganite thin-films for infrared detection and imaging," *Annalen der Physik*, vol. 13, pp. 48-51, 2004.

[6] J. Zhang, *et al.*, "Strain effect and the phase diagram of $La_{1-x}Ba_xMnO_3$ thin films," *Physical Review B*, vol. 64, p. 184404, 2001.

[7] T. Kanki, *et al.*, "Anomalous strain effect in $La_{0.8}Ba_{0.2}MnO_3$ epitaxial thin film: Role of the orbital degree of freedom in stabilizing ferromagnetism," *Physical Review B*, vol. 64, p. 224418, 2001.

[8] P. J. Wright, *et al.*, "Metal organic chemical vapor deposition (MOCVD) of oxides and ferroelectric materials," *Journal of Materials Science: Materials in Electronics*, vol. 13, pp. 671-678, 2002.

[9] V. Moshnyaga, *et al.*, "Preparation of rare-earth manganite-oxide thin films by metalorganic aerosol deposition technique," *Applied Physics Letters*, vol. 74, pp. 2842-2844, 1999.

[10] G. Koster, *et al.*, "Quasi-ideal strontium titanate crystal surfaces through formation of strontium hydroxide," *Applied Physics Letters*, vol. 73, pp. 2920-2922, 1998.

[11] J. S. Lee, *et al.*, "Hidden Magnetic Configuration in Epitaxial $La_{1-x}Sr_xMnO_3$ Films," *Physical Review Letters*, vol. 105, p. 257204, 2010.

[12] A. I. Tovstolytkin, *et al.*, "Complex phase separation in $La_{0.6}Ca_{0.4}MnO_3$ films revealed by electron spin resonance," *Physical Review B*, vol. 83, p. 184404, 2011.